



CHALMERS
UNIVERSITY OF TECHNOLOGY

Pilot-Assisted URLLC Links: Impact of Synchronization Error

Downloaded from: <https://research.chalmers.se>, 2025-02-22 19:49 UTC

Citation for the original published paper (version of record):

Kislal, A., Rajiv, M., Durisi, G. et al (2024). Pilot-Assisted URLLC Links: Impact of Synchronization Error. IEEE International Conference on Communications: 617-622.
<http://dx.doi.org/10.1109/ICC51166.2024.10623062>

N.B. When citing this work, cite the original published paper.

© 2024 IEEE. Personal use of this material is permitted. Permission from IEEE must be obtained for all other uses, in any current or future media, including reprinting/republishing this material for advertising or promotional purposes, or reuse of any copyrighted component of this work in other works.

Pilot-Assisted URLLC Links: Impact of Synchronization Error

A. Oguz Kislal¹, Madhavi Rajiv², Giuseppe Durisi¹, Erik G. Ström¹, Urbashi Mitra²

¹Chalmers University of Technology

²University of Southern California

Emails: kislal@chalmers.se, rajiv@usc.edu, {durisi, erik.strom}@chalmers.se, ubli@usc.edu

Abstract—We propose a framework to evaluate the random-coding union bound with parameter s (RCUs) on the achievable error probability in the finite-blocklength regime for a pilot-assisted transmission scheme operating over an imperfectly synchronized and memoryless block-fading waveform channel. Unlike previous results, which disregard the effects of imperfect synchronization, our framework utilizes pilots for both synchronization and channel estimation. Additionally, we utilize the saddlepoint approximation to provide a numerically efficient method for evaluating the RCUs bound in this scenario. Our numerical experiments verify the accuracy of the proposed approximation. Moreover, when transmission blocks are received synchronously, numerical results indicate that the number of pilot symbols needed to estimate the fading channel gains to the level of accuracy required in ultra-reliable low-latency communication is also sufficient to acquire sufficiently good synchronization. However, when the blocks are received asynchronously, there can be a significant SNR penalty compared to the synchronous case.

Index Terms—URLLC, pilots, synchronization, channel estimation

I. INTRODUCTION

Ultra-reliable low-latency communications (URLLC) are designed for mission-critical applications targeting 99.999% reliability with end-to-end latency as low as 1 ms [1]. A key feature of URLLC traffic is the frequent use of small information payloads accompanied by short packets consisting of a limited number of encoded symbols. In URLLC, there are limitations on the signal duration and available bandwidth, due to latency requirements and the need to orthogonalize multiple-user transmissions to mitigate multi-user interference. As a consequence, the conventional asymptotic performance metrics commonly employed in the design of communication systems, namely the ergodic and outage rates, are not suitable for the short-packet regime [2]. Because of its relevance for URLLC, the field of finite-blocklength information theory has been studied extensively, particularly following the seminal work [3], which offers a precise understanding of the tradeoff between error probability and packet size, for a given SNR and transmission rate, when operating with finite blocklengths.

In this paper, we focus on communication over memoryless block-fading channels with imperfect synchronization,

with the goal of understanding the impact of synchronization accuracy on the overall system performance. Benchmarking URLLC systems with such goals often requires the use of approximation techniques, due to the computational expense of evaluating finite blocklength bounds exactly.

The computationally efficient approximation proposed in this paper is based on the saddlepoint method [4], which is used to evaluate the random coding union bound with parameter s (RCUs) proposed in [5]. This bound is well-suited for communication over fading channels, as it can be applied to both the optimal non-coherent maximum-likelihood (ML) decoder and more practically significant decoders that utilize pilot-assisted transmission (PAT) [6]. Specifically, the decoder considered in this paper is the so-called scaled nearest-neighbor (SNN) decoder [7], which minimizes the error probability when synchronization and channel estimation is perfect, but is suboptimal otherwise. The evaluation of the RCUs bound for URLLC scenarios can be computationally expensive, and, for some applications, needs to be approximated by methods similar to the one proposed in this paper [8].

Most existing approaches for benchmarking URLLC systems disregard synchronization errors. In these approaches, an upper bound on the error probability is obtained by evaluating the tail probability of a sum of independent random variables. This allows for approximations such as the *normal approximation* [3], or the more accurate *saddlepoint approximation* [9, Ch. XVI], [4, Ch. 6]. The saddlepoint approximation has been applied to the case of an optimal ML decoder in [10], of PAT transmission and SNN decoding over single-input single-output (SISO) and multiple-input multiple-output (MIMO) channels in [11], and of PAT transmission and SNN decoding over massive MIMO for both single and multiple fading blocks in [6], [8], [12]. In [13], the problem of joint synchronization and decoding is analyzed from a finite-blocklength perspective. There, it is shown that one can achieve performance close to the perfectly synchronized case even for an exponentially large asynchronism level. However, asynchronism is modeled only at symbol level, and imperfect synchronization results only in a wrong estimate of the location of the transmitted codeword.

In this paper, we consider the more practically relevant case in which asynchronism is modeled on the waveform channel, and imperfect synchronization yields also intersymbol interference after matched filtering and sampling. As we shall see,

This work has been funded in part by one or more of the following grants: NSF CCF-1817200, DOE DE-SC0021417, Swedish Research Council 2018-04359 and 2021-04970, NSF CCF-2008927, NSF CCF-2200221, ONR 503400-78050, ONR N00014-15-1-2550

this implies that the random variables that need to be analyzed to obtain upper bounds on the error probability are, in general, dependent, and the saddlepoint approximations provided in [6], [8], [11], [12] are therefore not applicable. However, under certain assumptions on the dependence between the random variables, saddlepoint approximations can still be derived.

Contributions: We consider the problem of transmitting short packets over a SISO memoryless block-fading waveform channel with an unknown delay and analyze the impact of imperfect synchronization and channel estimation on system performance in the URLLC regime. Specifically, we design a synchronization and channel estimation algorithm that can be used both in cases of asynchronous and synchronous reception of the fading blocks. We use the RCUs bound for the case of PAT and SNN decoding to evaluate the error probability achievable when using this (or any other) algorithm, and also provide a novel saddlepoint approximation for this bound, based on [4, Ch. 6], which is tailored to the specific dependence between random variables that arises due to imperfect synchronization. Finally, we provide numerical results to illustrate the accuracy of the proposed approximation and its usefulness in obtaining insights into the design of URLLC links.

Notation: We denote random vectors and random scalars by upper-case boldface letters such as \mathbf{X} and upper-case standard letters, such as X , respectively. Their realizations are indicated by lower-case letters of the same font. To avoid ambiguities, we use another font, such as \mathbb{R} for rate, to denote constants that are typically capitalized in the literature. The circularly symmetric Gaussian distribution is denoted by $\mathcal{CN}(\mu, \sigma^2)$, where μ and σ^2 denote the mean and the variance, respectively. The superscripts $(\cdot)^T$ and $(\cdot)^H$ denote transposition and Hermitian transposition, respectively. We write $\log(\cdot)$ to denote the natural logarithm, $\|\cdot\|$ stands for the ℓ^2 -norm, $\mathbb{P}[\cdot]$ for the probability of an event, $\mathbb{E}[\cdot]$ for the expectation operator, $*$ for the convolution operation, $Q(\cdot)$ for the Gaussian Q -function, and \mathbf{I}_m for the $m \times m$ identity matrix, respectively. Finally, for two functions $f(n)$ and $g(n)$, the notation $f(n) = o(g(n))$ means that $\lim_{n \rightarrow \infty} f(n)/g(n) = 0$ and the notation $f(n) = \mathcal{O}(g(n))$ means that $\limsup_{n \rightarrow \infty} |f(n)/g(n)| < \infty$.

II. SYSTEM MODEL

We consider pilot-assisted transmission of a uniformly distributed message over a SISO block-flat-fading channel with unknown delay. The message to be transmitted is encoded using a codebook \mathcal{C} containing $\lceil \exp(n_b(n_p + n_s)\mathbb{R}) \rceil$ codewords, where n_b is the number of available fading blocks, n_p and n_s are the number of pilot and data symbols in each block, respectively, and \mathbb{R} is the data transmission rate in nats per channel use. Each codeword is the concatenation of n_b subcodewords, each comprising n_s symbols.

We transmit vectors with length $n_c = n_s + n_p$ over each of the n_b independent block-fading channels, with a pilot vector inserted at the beginning of each subcodeword. The channel gain is assumed to remain constant during the transmission of a vector. At the receiver, we perform synchronization and

estimate the channel using the pilot symbols. The decoder output is the codeword in the codebook that, after being scaled with the channel estimate, is closest to the received vector, sampled using the delay estimate, in Euclidean distance.

A. Signal Model

The n_p symbols within each transmitted vector are used to form the continuous-time pilot signal $x^{(p)}(t)$ as follows

$$x^{(p)}(t) = \sum_{k=1}^{n_p} x_k^{(p)} s_{t_p}(t - (k-1)t_p), \quad (1)$$

where $x_k^{(p)}$ are deterministic symbols known to the receiver with symbol energy $\rho = |x_k^{(p)}|^2$, and $s_{t_p}(t)$ is a square pulse with normalized energy and support of size t_p , i.e.,

$$s_{t_p}(t) \doteq \begin{cases} \frac{1}{\sqrt{t_p}}, & t \in [0, t_p) \\ 0, & \text{otherwise} \end{cases}. \quad (2)$$

The data symbols for the ℓ th fading block are sent after the pilot symbols via the continuous-time signal

$$x_\ell^{(d)}(t) = \sum_{k=1}^{n_s} x_{k,\ell}^{(d)} s_{t_p}(t - (k-1)t_p - n_p t_p), \quad (3)$$

where $x_{k,\ell}^{(d)}$ is the k th data symbol of the ℓ th fading block, with average energy ρ . The total continuous-time signal corresponding to the ℓ th vector is put through a flat-fading channel to obtain the received continuous signal

$$Y_\ell(t) = H_\ell \left(x^{(p)}(t - D_\ell) + x_\ell^{(d)}(t - D_\ell) \right) + Z_\ell(t), \quad (4)$$

where H_ℓ denotes the scalar random fading complex channel gain for the ℓ th fading block, D_ℓ is the time delay for the ℓ th fading block, which we assume to be uniform in $[0, d_{\max}]$, and $Z_1(t), \dots, Z_{n_b}(t)$ are independent white complex Gaussian processes with power spectral density N_0 . For simplicity, we set $N_0 = 1$.

Depending on the communication system, the receiver may or may not receive all $\mathbf{Y}_\ell(t)$ synchronously.¹ We therefore distinguish between the asynchronous case where D_1, \dots, D_{n_b} are i.i.d. and the synchronous case where $D_1 = \dots = D_{n_b} = D$. In the former case, information about the pair (D_ℓ, H_ℓ) is found only in $Y_\ell(t)$, and the estimation problem decouples into n_b separate problems, one per block. However, in the synchronous case, it will be advantageous to jointly estimate (D, H_1, \dots, H_{n_b}) . We next introduce synchronization and channel estimation algorithms for both cases.

B. Synchronization and Channel Estimation Phase

The receiver uses the knowledge of the pilot sequence to estimate the propagation delays and the fading-block gains. Throughout, we assume that the receiver employs synchronization and channel estimation algorithms that take an upsampled

¹For example, all $\mathbf{Y}_\ell(t)$ are typically received synchronously when frequency diversity is used, while asynchronous reception occurs when different $\mathbf{Y}_\ell(t)$ experience different delays due to the medium access protocol.

version of the received signal as the input. For a given upsampling rate N , let t_s be the sampling interval; then, $t_p = t_s N$ is the period of the pulses used to construct the continuous time pilot and data signals. We also let $x_{N,n}^{(p)} = x_{\lfloor n/N \rfloor}^{(p)}$ be the n th element of the upsampled vector of pilot symbols, where $n = 1, \dots, Nn_p$. In order to obtain an upsampled received signal, we process and sample the received signal $Y_\ell(t)$ as

$$Y_{m,\ell}^{(p)} = (Y_\ell * s_{t_s})(mt_s), \quad (5)$$

where $m = 1, \dots, M$, and the sampling endpoint is chosen to capture all pilot symbols as $M = \lceil d_{\max}/t_s \rceil + n_p N$.

We can now represent the upsampled signal vector as

$$\mathbf{Y}_\ell^{(p)} = H_\ell \begin{bmatrix} \mathbf{x}_N^{(p)}(Q_\ell) & \mathbf{x}_N^{(p)}(Q_\ell + 1) \end{bmatrix} \begin{bmatrix} 1 - \frac{E_\ell}{t_s} \\ \frac{E_\ell}{t_s} \end{bmatrix} + \mathbf{Z}_\ell + \mathbf{C}_\ell \quad (6)$$

where $Q_\ell \doteq \lfloor D_\ell/t_s \rfloor$, $E_\ell \doteq D_\ell - Q_\ell t_s$,

$$\mathbf{x}_N^{(p)}(q_\ell) \doteq \frac{1}{\sqrt{N}} \left[\mathbf{0}_{q_\ell}^T, x_{N,1}^{(p)}, \dots, x_{N,Nn_p}^{(p)}, \mathbf{0}_{M-q_\ell-Nn_p}^T \right]^T, \quad (7)$$

$\mathbf{Y}_\ell^{(p)} \doteq [Y_{1,\ell}^{(p)}, \dots, Y_{M,\ell}^{(p)}]^T$, $\mathbf{Z}_\ell \sim \mathcal{CN}(\mathbf{0}_M, \mathbf{I}_M)$, and \mathbf{C}_ℓ stands for the interference from the data signal. We note that $D_\ell = Q_\ell t_s + E_\ell$, where $Q_\ell \in \mathbb{Z}$ and $E_\ell \in [0, t_s)$.

For simplicity, our algorithms are derived by considering the ML estimators of the parameters in question in the case where $\mathbf{C}_\ell = \mathbf{0}_M$, i.e., where no interference from the data symbols is present. As we shall verify in Section IV, our assumption incurs minimal loss.

1) Per-Block Synchronization for Asynchronous Reception:

In this case, the receiver uses the observation of $\mathbf{Y}_\ell^{(p)}$ for each fading block in order to obtain the estimates \hat{H}_ℓ , \hat{Q}_ℓ , and \hat{E}_ℓ . To do so, we pose the following minimization problem:

$$[\hat{H}_\ell, \hat{Q}_\ell, \hat{E}_\ell] = \arg \min_{\hat{h}, \hat{q}, \hat{e}} \|\mathbf{Y}_\ell^{(p)} - \bar{h} \mathbf{v}(\hat{q}, \hat{e})\|^2, \quad (8)$$

where

$$\mathbf{v}(\bar{q}, \bar{e}) \doteq \begin{bmatrix} \mathbf{x}_N^{(p)}(\bar{q}) & \mathbf{x}_N^{(p)}(\bar{q} + 1) \end{bmatrix} \begin{bmatrix} 1 - \frac{\bar{e}}{t_s} \\ \frac{\bar{e}}{t_s} \end{bmatrix}. \quad (9)$$

For any given $\mathbf{Y}_\ell^{(p)} = \mathbf{y}_\ell^{(p)}$, the ML channel estimate for each fading block \hat{h}_ℓ can be written as a function of \bar{q} and \bar{e} as

$$\hat{h}_\ell(\bar{q}, \bar{e}) = \frac{\mathbf{v}(\bar{q}, \bar{e})^H \mathbf{y}_\ell^{(p)}}{\|\mathbf{v}(\bar{q}, \bar{e})\|^2}. \quad (10)$$

Substituting (10) into (8), we can estimate the delay parameters as [14]

$$[\hat{q}_\ell, \hat{e}_\ell] = \arg \max_{\bar{q}, \bar{e}} \frac{n(\bar{q}, \bar{e})}{d(\bar{q}, \bar{e})}, \quad (11)$$

where $n(\bar{q}, \bar{e}) = \left| \mathbf{v}(\bar{q}, \bar{e})^H \mathbf{y}_\ell^{(p)} \right|^2$ and $d(\bar{q}, \bar{e}) = \|\mathbf{v}(\bar{q}, \bar{e})\|^2$. The maximization in (11) follows from substituting the expression for \hat{h}_ℓ in (10), for \bar{h}_ℓ in (8), and then expanding out terms and removing terms not dependent on \bar{q} and \bar{e} from the objective function.

For a fixed value of \bar{q} , both $n(\bar{q}, \bar{e})$ and $d(\bar{q}, \bar{e})$ are second-degree polynomials in \bar{e} , which implies that the objective

function in (11) is a rational function in \bar{e} . For a fixed value of \bar{q} , we find an extreme point of this function by differentiating with respect to \bar{e} and setting the derivative to zero as

$$\frac{\partial n(\bar{q}, \bar{e})}{\partial \bar{e} d(\bar{q}, \bar{e})} = \frac{n'(\bar{q}, \bar{e})d(\bar{q}, \bar{e}) - n(\bar{q}, \bar{e})d'(\bar{q}, \bar{e})}{d(\bar{q}, \bar{e})^2} = 0. \quad (12)$$

If (12) has a solution \bar{e}^* in the range $(0, t_s)$, then (\bar{q}, \bar{e}^*) is a candidate for $(\hat{q}_\ell, \hat{e}_\ell)$. We also consider the boundary points $(\bar{q}, 0)$ and (\bar{q}, t_s) since they might be the solution of (12) in the cases where no extreme point can be found in $(0, t_s)$, or when a minimum point (instead of a maximum) is found.

We are now ready to introduce our delay and channel estimation algorithm. Let \mathcal{D}_ℓ be the set of candidates for $\hat{d}_\ell = \hat{q}_\ell t_s + \hat{e}_\ell$. We construct \mathcal{D}_ℓ as follows: for each $\bar{q} \in \{0, \dots, d_{\max}/t_s\}$ we add $\bar{q}t_s$ to \mathcal{D}_ℓ . Next, we find the solutions \bar{e}^* for (12) for each \bar{q} . If \bar{e}^* is in the range $[0, t_s)$, we add $\bar{q}t_s + \bar{e}^*$ to \mathcal{D}_ℓ . We then find \hat{d}_ℓ as the entry in \mathcal{D}_ℓ that maximizes the objective function in (11). This estimate is then used to evaluate the channel estimate \hat{h}_ℓ from (10).

2) *Joint Synchronization for Synchronous Reception:* In this case, since the delay is same for all fading blocks (i.e., $D_\ell = D$ for all ℓ), the receiver can use the observations of $\{\mathbf{Y}_\ell^{(p)}\}_{\ell=1}^{n_b}$ jointly. These observations are used to estimate the channel gains $\hat{\mathbf{H}} = [\hat{H}_1, \dots, \hat{H}_{n_b}]^T$ and delay as

$$[\hat{\mathbf{H}}, \hat{Q}, \hat{E}] = \arg \min_{\hat{\mathbf{h}}, \hat{q}, \hat{e}} \sum_{\ell=1}^{n_b} \|\mathbf{Y}_\ell^{(p)} - \bar{h}_\ell \mathbf{v}(\hat{q}, \hat{e})\|^2. \quad (13)$$

Following the same steps leading to (11), we obtain

$$[\hat{q}, \hat{e}] = \arg \max_{\bar{q}, \bar{e}} \sum_{\ell=1}^{n_b} \frac{|\mathbf{v}(\bar{q}, \bar{e})^H \mathbf{y}_\ell|^2}{\|\mathbf{v}(\bar{q}, \bar{e})\|^2}. \quad (14)$$

The numerator and denominator of (14) have the same polynomial structure as (11), and the same synchronization and channel estimation algorithm described in Section II-B1 can be used, but now with only one set of candidates \mathcal{D} .

C. Codeword Decoding Phase

The codeword decoding phase is based on a mismatch-decoding approach, where the delay and channel estimates returned by the algorithms described in Section II-B are treated as perfect. The input-output relationship for the k th symbol in the ℓ th block, assuming that the synchronization is not off by more than one symbol (i.e., $|\hat{D} - D| \leq t_p$) is²

$$Y_{k,\ell} = (Y_\ell * s_{t_p})(kt_p + n_p t_p + \hat{D}_\ell) \quad (15)$$

In the decoding process, the receiver seeks the codeword in the codebook \mathcal{C} closest to the received signal after scaling each subcodeword with the corresponding channel estimate. Hence, given the received vector and the channel estimates, the decoded codeword $\hat{\mathbf{x}} = [\hat{\mathbf{x}}_1^T, \dots, \hat{\mathbf{x}}_{n_b}^T]^T$ is determined as

$$\hat{\mathbf{x}} = \arg \min_{\bar{\mathbf{x}} = [\bar{\mathbf{x}}_1, \dots, \bar{\mathbf{x}}_{n_b}] \in \mathcal{C}} \sum_{\ell=1}^{n_b} \|\mathbf{y}_\ell - \hat{h}_\ell \bar{\mathbf{x}}_\ell\|^2, \quad (16)$$

²We will omit the superscript (d) in the remainder of the paper to keep the notation compact.

where $\mathbf{y}_\ell = [y_{1,\ell}, \dots, y_{n_s,\ell}]^T$ and $\bar{\mathbf{x}}_\ell$ is defined similarly. This decoder, known as the *mismatched SNN decoder* [15], is not optimal. However, it is practically relevant and the analysis of its finite-blocklength error probability is tractable [6].

III. A NON-ASYMPTOTIC UPPER BOUND ON THE ERROR PROBABILITY

We may evaluate the packet error probability ϵ_{pep} as

$$\epsilon_{\text{pep}} = \mathbb{P}\left[\left|\hat{D}_\ell - D_\ell\right| \leq t_p\right] \epsilon_1 + \mathbb{P}\left[\left|\hat{D}_\ell - D_\ell\right| > t_p\right] \epsilon_2, \quad (17)$$

where ϵ_1 and ϵ_2 are the probability of erroneous packet decoding when the synchronization is off by less than and more than one symbol, respectively. When evaluating ϵ_{pep} , we will assume, for simplicity, that the decoder cannot decode the packet when synchronization is off more than one symbol, i.e., we will set $\epsilon_2 = 1$.

In the next section, we will present an RCUs bound for ϵ_1 and its corresponding saddlepoint approximation.

A. The RCUs Finite-Blocklength Bound

The RCUs bound is obtained by a random-coding argument. This means that instead of analyzing the performance of a particular code, we evaluate the average error probability averaged over a randomly constructed ensemble of codebooks. In this paper, we consider an i.i.d. discrete ensemble in which each symbol of every codeword is drawn independently (and uniformly) from a constellation set with u elements (e.g., $u = 2$ for BPSK) and power ρ . Although potentially suboptimal, this choice is practically relevant and allows us to evaluate the RCUs bound efficiently via a saddlepoint approximation.

When the synchronization is off by less than one symbol (i.e., $|\hat{D}_\ell - D_\ell| \leq t_p$), (15) can be stated as

$$Y_{k,\ell} = H_\ell(\Delta_\ell X_{k,\ell} + (1 - \Delta_\ell)X_{k+\Lambda_\ell,\ell}) + Z_{k,\ell}, \quad (18)$$

where we define $\Delta_\ell \doteq 1 - |\hat{D}_\ell - D_\ell|/t_p$, $\Lambda_\ell \doteq \text{sign}(\hat{D}_\ell - D_\ell)$, and $Z_{k,\ell}$ are i.i.d. zero-mean, unit-variance, complex Gaussian random variables. Note that the lack of perfect synchronization, i.e., $\Delta_\ell \neq 1$, yields intersymbol interference.

For our setup, the RCUs achievability bound ϵ_{ub} on ϵ_1 is given by $\epsilon_1 \leq \epsilon_{\text{ub}}$ with

$$\epsilon_{\text{ub}} = \mathbb{E}_{\mathbf{H}, \hat{\mathbf{H}}, \Delta} \left[\epsilon_{\text{ub}}(\mathbf{H}, \hat{\mathbf{H}}, \Delta) \right] \quad (19)$$

where $\mathbf{H} = [H_1, \dots, H_{n_b}]^T$, $\Delta = [\Delta_1, \dots, \Delta_{n_b}]^T$, and

$$\begin{aligned} \epsilon_{\text{ub}}(\mathbf{h}, \hat{\mathbf{h}}, \delta) &= \mathbb{P} \left[\frac{\log \Upsilon}{n_c n_b} + \frac{1}{n_c n_b} \sum_{\ell=1}^{n_b} \sum_{k=1}^{n_s} \iota_s(X_{k,\ell}; Y_{k,\ell}, \hat{h}_\ell) \right. \\ &\quad \left. \leq R \mid \mathbf{H} = \mathbf{h}, \hat{\mathbf{H}} = \hat{\mathbf{h}}, \Delta = \delta \right]. \quad (20) \end{aligned}$$

Here, Υ is a random variable that is uniformly distributed on $[0, 1]$ and independent of all other quantities, and $\iota_s(x, y, \hat{h})$ is the so-called *generalized information density* [5]

$$\iota_s(x; y, \hat{h}) \doteq \log \frac{e^{-s|y - \hat{h}x|^2}}{\mathbb{E}_{\bar{X}} \left[e^{-s|y - \hat{h}\bar{X}|^2} \right]}, \quad (21)$$

where \bar{X} is independent of all other random variables and drawn uniformly from the constellation, and $s > 0$ is a parameter that can be optimized to obtain a tighter bound. No closed-form expression for the RCUs bound (19) is, in general available. Numerical methods to evaluate it, such as Monte-Carlo simulations, can be time consuming due to the low target error probabilities of interest in URLLC. Next, we introduce a saddlepoint approximation of (19) that allows for an efficient computation.

B. A Saddlepoint Approximation on (20)

The saddlepoint method is a well-established tool to obtain accurate approximations of tail probabilities involving sum of random variables. Unfortunately, none of the saddlepoint approximations for the RCUs bounds reported previously in the literature [6], [8], [11], [12] apply to the setup considered in this paper (see [14] for a detailed discussion). To obtain the desired saddlepoint approximation, we exploit the property that the random variables $\{\sum_{k=1}^{n_s} \iota_s(X_{k,\ell}; Y_{k,\ell}, \hat{h}_\ell)\}_{\ell=1}^{n_b}$ are conditionally independent, given $\mathbf{H} = \mathbf{h}$, $\hat{\mathbf{H}} = \hat{\mathbf{h}}$, and $\Delta = \delta$. This allows us to perform a saddlepoint expansion of the conditional error probability in (20) with respect to the number of blocks n_b . Specifically, let us fix δ , \mathbf{h} , and $\hat{\mathbf{h}}$, and denote for convenience $I_\ell \doteq \sum_{k=1}^{n_s} \iota_s(X_{k,\ell}; Y_{k,\ell}, \hat{h}_\ell)$. Note that $\{I_\ell\}_{\ell=1}^{n_b}$ is a family of independent, but not necessarily identically distributed random variables.

Let us denote by $\varphi_\ell(\zeta) = \mathbb{E}[e^{-\zeta I_\ell}]$ the MGF of $-I_\ell$ and by $\kappa_\ell(\zeta) = \log \varphi_\ell(\zeta)$ its cumulant generating function (CGF). Let us also set $\kappa(\zeta) = \sum_{\ell=1}^{n_b} \kappa_\ell(\zeta)$ as well as $\mu(\zeta) \doteq \frac{1}{n_b} \frac{d\kappa(\zeta)}{d\zeta}$ and $\sigma^2(\zeta) \doteq \frac{1}{n_b} \frac{d^2 \kappa(\zeta)}{d\zeta^2}$. In the next theorem, we present a saddlepoint approximation on (20) (see [14, Thm. 1] for its proof).

Theorem 1: Suppose that there exists a $\zeta_0 > 0$ such that

$$\sup_{|\zeta| < \zeta_0} \left| \frac{d^4 \varphi_\ell(\zeta)}{d\zeta^4} \right| < \infty, \quad \forall \ell \in \{1, \dots, n_b\} \quad (22)$$

and also positive constants $m_l \leq m_u$ such that

$$m_l \leq \sigma^2(\zeta) \leq m_u \quad (23)$$

holds for all $n_b \in \mathbb{N}$ and for all $|\zeta| \leq \zeta_0$. Assume that there exists a $\zeta \in [-\zeta_0, \zeta_0]$ satisfying $-\mu(\zeta) = n_c R$. If $\zeta \in [0, 1]$ then

$$\begin{aligned} &\mathbb{P} \left[\log \Upsilon + \sum_{\ell=1}^{n_b} I_\ell \leq n_b n_c R \right] \\ &= e^{\kappa(\zeta) - n_b \zeta \mu(\zeta)} \left[e^{\frac{\beta_\zeta^2}{2}} Q(\beta_\zeta) + e^{\frac{\beta_{1-\zeta}^2}{2}} Q(\beta_{1-\zeta}) + o\left(\frac{1}{\sqrt{n_b}}\right) \right] \quad (24) \end{aligned}$$

where $\beta_a = a\sqrt{n_b \sigma^2(\zeta)}$. If $\zeta > 1$, then

$$\begin{aligned} &\mathbb{P} \left[\log \Upsilon + \sum_{\ell=1}^{n_b} I_\ell \leq n_b n_c R \right] \\ &= e^{\kappa(1) - n_b \mu(\zeta)} \left[\Psi_{n_b}(1, 1) - \Psi_{n_b}(0, -1) + \mathcal{O}\left(\frac{1}{\sqrt{n_b}}\right) \right] \quad (25) \end{aligned}$$

where

$$\Psi_{n_b}(a, b) = e^{n_b a [-\mu(1) - n_c R + \sigma^2(1)/2]} \times Q\left(a\sqrt{n_b\sigma^2(1)} - b\frac{n_b(\mu(1) + n_c R)}{\sqrt{n_b\sigma^2(1)}}\right). \quad (26)$$

Finally, if $\zeta < 0$, then

$$\mathbb{P}\left[\log \Upsilon + \sum_{\ell=1}^{n_b} I_\ell \leq n_b n_c R\right] = 1 - \left(e^{\kappa(\zeta) - n_b \zeta \mu(\zeta)}\right) \times \left[e^{\frac{\beta^2 \zeta}{2}} Q(\beta_{-\zeta}) - e^{\frac{\beta^2 - \zeta}{2}} Q(\beta_{1-\zeta}) + \mathcal{O}\left(\frac{1}{\sqrt{n_b}}\right)\right]. \quad (27)$$

The saddlepoint approximation is then obtained by neglecting the $o(\cdot)$ and $\mathcal{O}(\cdot)$ terms in (24), (25), and (27).

The main challenge when using this approximation is to evaluate the MGF $\varphi_\ell(\zeta) = \mathbb{E}[e^{-\zeta I_\ell}]$, which is required to determine $\kappa(\zeta)$ and its first and second derivatives. Note that each I_ℓ consists of the sum of n_s random variables that, in general, are dependent due to the intersymbol interference caused by errors in the estimation of the propagation delay. Inspired by [4, Ch. 9], we exploit the Markovian structure of the dependence between these random variables to evaluate $\varphi_\ell(\zeta)$ efficiently. The details of this evaluation can be found in [14].

IV. NUMERICAL RESULTS AND DISCUSSION

In this section, we report numerical experiments illustrating the performance of our synchronization method both in terms of normalized mean square error (NMSE) and achievable packet error probability. We also verify the accuracy of the saddlepoint approximation.

Throughout, we shall consider the synchronous reception case; we shall also assume that a BPSK constellation is used for both pilot and data transmission, and that m-sequences [16, Ch. 8] are used as pilot sequences. We assume that the H_ℓ , $\ell = 1, \dots, n_b$, are generated independently from a $\mathcal{CN}(0, 1)$ distribution. We will analyze the performance of both the per-block and the joint synchronization algorithms proposed in Section II-B. Note that per-block synchronization, when applied to synchronous reception, achieves the same performance as if the blocks were received asynchronously.

We first compare the NMSE incurred when estimating D with both the joint synchronization and per-block synchronization. The NMSE for joint synchronization is $\mathbb{E}[(D - \hat{D})^2/t_p^2]$, and for per-block synchronization, the NMSE is $\mathbb{E}[(D_\ell - \hat{D}_\ell)^2/t_p^2]$ (which does not depend on ℓ). In Fig. 1, we plot the NMSE as a function of the SNR for the case $N = 20$, $n_b = 4$, and $n_p = 7$. Recall that both per-block and joint synchronizations were developed by considering the ML estimators under the assumption that $\mathbf{C}_\ell = \mathbf{0}_M$. In Fig. 1, we plot the NMSE for the delay estimation as a function of the SNR for both the case of no data interference ($\mathbf{C}_\ell = \mathbf{0}_M$) and data interference. We observe that joint synchronization performs significantly better than per-block synchronization. The gap in performance between joint

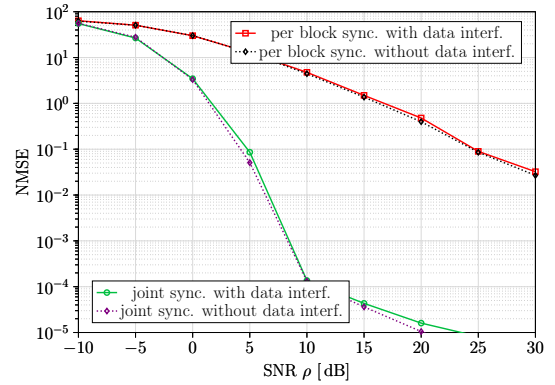


Fig. 1. NMSE for the delay estimation for both joint and per-block synchronization for $N = 20$, $n_b = 4$, $n_p = 7$.

and per-block synchronization is small at very low SNR, but the performance gap increases as SNR increases, as expected. We also observe that the impact of data interference on the performance of our algorithm is minimal.³

In Fig. 2, we illustrate the impact of synchronization errors on the packet error probability, upper bounded by substituting the RCUs bound ϵ_{ub} for ϵ_1 and setting $\epsilon_2 = 1$ in (17). To do so, we let σ_d^2 be the mean squared error incurred when estimating D . In this analysis (and only in this analysis), we assume the channel to be known at the receiver (i.e., $\hat{h}_\ell = h_\ell$ for all ℓ), let $\hat{D} \sim \mathcal{N}(D, \sigma_d^2)$ (or $\hat{D}_\ell \sim \mathcal{N}(D, \sigma_d^2)$ for the per-block synchronization algorithm), where we allow σ_d^2 , which corresponds to the mean square error for delay estimation, to vary independently from any other system parameter, and report an upper bound on the ϵ_{pep} as a function of σ_d^2/t_p^2 for $\rho \in \{2.5, 6.5\}$ dB, $n_b n_c = 288$, $n_b = 8$, $n_p = 0$, and $R = 30/288 = 0.104$ bit per channel use. The parameter s of the RCUs bound is optimized. Note that, since we assumed that the $\{h_\ell\}$ are known to the receiver, once we fix σ_d^2 , the packet error probability achieved using joint synchronization and per-block synchronization coincide. We see from the figure that to achieve an error probability $\epsilon_{pep} < 10^{-4}$ for both values of ρ , it is enough that σ_d^2/t_p^2 is below 0.12 and that the error probability deteriorates rapidly once this value is exceeded.

Finally, we analyze in Fig. 3 the performance achievable in the URLLC regime using the synchronization and channel estimation algorithms introduced in Section II-B. Specifically, we show the SNR sufficient to achieve an error probability of 10^{-5} for $n_b n_c = 288$, $N = 20$, and $R = 0.104$ bit per channel, as a function of the number of fading blocks n_b spanned by each codeword. We obtain each value of SNR by optimizing over both the number of pilot symbols n_p and the s parameter in the RCUs. We consider both per-block and joint synchronization, and depict for reference also the curve corresponding to perfect synchronization, but pilot-aided estimation of the channel gain. For each scenario, we plot

³In [14], we also show that the NMSE for both synchronization methods approaches the corresponding Cramér-Rao lower bounds.

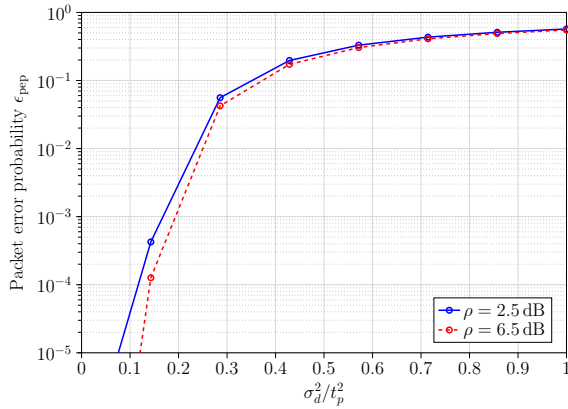


Fig. 2. Achievable packet error probability evaluated using the RCUs bound as a function of the average synchronization error. Here $n = 288$, $n_b = 8$, $R = 0.104$ bit per channel use; s is optimized.

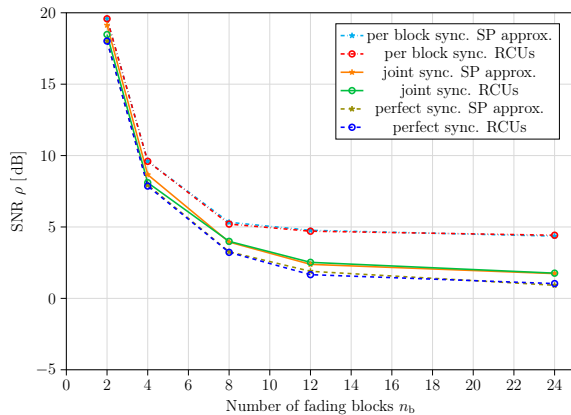


Fig. 3. Upper bound on the SNR sufficient to achieve $\epsilon_{ub} = 10^{-5}$ as a function of n_b . Here, $n_b n_c = 288$, $R = 0.104$ bit per channel use, $N = 20$; n_p and s are optimized.

both the RCUs and its saddlepoint approximation. We observe that the saddlepoint approximation provides an accurate and numerically efficient approximation of the RCUs bound for the parameters considered in the figure. This also suggests that the conditions required for the saddlepoint approximation, given in (22) and (23), hold in our setup.

We observe from the figure that per-block synchronization requires up to 3.5 dB higher SNR than joint synchronization to achieve the same error probability. We note that when $n_b \geq 4$, the SNR gap between joint synchronization and perfect synchronization but pilot-aided channel estimation is no larger than 0.6 dB. This suggests that the pilot symbols needed to estimate the fading coefficients in the perfect synchronization, pilot-aided channel estimation case are sufficient to also estimate the delay when the joint synchronization algorithm is used.

V. CONCLUSIONS

We have presented an efficient method to evaluate an upper bound on the error probability achievable over memoryless block-fading channels, with pilot-assisted transmission for

channel estimation and synchronization. The method is based on a novel saddlepoint approximation, which accounts for the dependence across certain random variables arising in the presence of synchronization errors.

Numerical experiments show that the proposed saddlepoint approximation can be safely used to benchmark practically relevant URLLC systems. We show how to use our approximation to determine the synchronization level required to achieve the low error probabilities demanded in URLLC applications. Moreover, our numerical results reveal that, when the fading blocks are received synchronously and synchronization is performed jointly over the blocks, the pilot symbols needed for channel estimate are sufficient to acquire synchronization. However, if we use per-block synchronization (which is unavoidable in the asynchronous case), there can be a significant SNR penalty compared to the joint synchronization case.

REFERENCES

- [1] "Study on physical layer enhancements for NR ultra-reliable and low latency case (URLLC) (release 16)," 3GPP, Tech. Rep., Mar. 2019. [Online]. Available: <https://portal.3gpp.org/desktopmodules/Specifications/SpecificationDetails.aspx?specificationId=3498>
- [2] G. Durisi, T. Koch, and P. Popovski, "Towards massive, ultra-reliable, and low-latency wireless communication with short packets," *Proc. IEEE*, vol. 104, no. 9, pp. 1711–1726, Sep. 2016.
- [3] Y. Polyanskiy, H. V. Poor, and S. Verdú, "Channel coding rate in the finite blocklength regime," *IEEE Trans. Inf. Theory*, vol. 56, no. 5, pp. 2307–2359, May 2010.
- [4] J. L. Jensen, *Saddlepoint Approximations*. Oxford, U.K.: Oxford Univ. Press, 1995.
- [5] A. Martínez and A. Guillén i Fàbregas, "Saddlepoint approximation of random-coding bounds," in *Proc. Inf. Theory Appl. Workshop*, San Diego, CA, USA, Feb. 2011, pp. 257–262.
- [6] J. Östman, G. Durisi, E. G. Ström, M. C. Coşkun, and G. Liva, "Short packets over block-memoryless fading channels: Pilot-assisted or noncoherent transmission?" *IEEE Trans. Commun.*, vol. 67, no. 2, pp. 1521–1536, Feb. 2019.
- [7] A. Lapidoth and S. Shamai (Shitz), "Fading channels: how perfect need "perfect side information" be?" *IEEE Trans. Inf. Theory*, vol. 48, no. 5, pp. 1118–1134, May 2002.
- [8] A. O. Kislal, A. Lancho, G. Durisi, and E. G. Ström, "Efficient evaluation of the error probability for pilot-assisted URLLC with massive MIMO," *IEEE J. Sel. Areas Commun.*, vol. 41, no. 7, pp. 1969–1981, May 2023.
- [9] W. Feller, *An Introduction to Probability Theory and Its Applications*. New York, NY, USA: Wiley, 1971, vol. 2.
- [10] A. Lancho, J. Östman, G. Durisi, T. Koch, and G. Vazquez-Vilar, "Saddlepoint approximations for short-packet wireless communications," *IEEE Trans. Wireless Commun.*, vol. 19, no. 7, pp. 4831–4846, Jul. 2020.
- [11] G. C. Ferrante, J. Östman, G. Durisi, and K. Kittichokechai, "Pilot-assisted short-packet transmission over multiantenna fading channels: A 5G case study," in *Proc. Conf. on Inf. Sci. and Sys. (CISS)*, Princeton, NJ, U.S.A., Mar. 2018, pp. 1–6.
- [12] J. Östman, A. Lancho, G. Durisi, and L. Sanguinetti, "URLLC with massive MIMO: Analysis and design at finite blocklength," *IEEE Trans. Wireless Commun.*, vol. 20, no. 10, pp. 6387–6401, Oct. 2021.
- [13] Y. Polyanskiy, "Asynchronous communication: Exact synchronization, universality, and dispersion," *IEEE Trans. Inf. Theory*, vol. 59, no. 3, pp. 1256–1270, 2013.
- [14] A. O. Kislal, M. Rajiv, G. Durisi, E. G. Ström, and U. Mitra, "Is synchronization a bottleneck for pilot-assisted URLLC links?" 2024. [Online]. Available: <https://arxiv.org/abs/2401.09089>
- [15] J. Scarlett, A. Martínez, and A. Guillén i Fàbregas, "Mismatched decoding: Error exponents, second-order rates and saddlepoint approximations," *IEEE Trans. Inf. Theory*, vol. 60, no. 5, pp. 2647–2666, May 2014.
- [16] J. G. Proakis, *Digital Communications*, 4th ed. Boston, MA, USA: McGraw-Hill, 2008.